

Limnological responses to warming on the Xizang Plateau, Tibet, over the past 200 years

Rong Wang · Xiangdong Yang · Peter Langdon · Enlou Zhang

Received: 8 June 2010 / Accepted: 3 January 2011 / Published online: 20 January 2011
© Springer Science+Business Media B.V. 2011

Abstract Paleolimnological analyses can be used to evaluate limnological responses to changing climate over decadal to centennial timescales, especially in regions with sparse lake monitoring data. We used a training set with 90 lakes to develop a diatom-based conductivity transfer function and address climate-driven changes in lakes on the Qinghai-Xizang Plateau, Tibet. This new training set is an expanded version of a previous model (Yang et al. in J Paleolimnol 30:1–19, 2003) and shows improved performance statistics for the conductivity model. The expanded training set also contains diatom species not previously identified from the region, such as *Stephanodiscus* sp. and *Cyclotella* sp., which are common eutrophic indicator species in other regions, but can also be influenced by water column conductivity. The new conductivity transfer function was applied to Lakes Nam Co and Chen Co in

Tibet. Recent conductivity inferences were compared with climate data from the Dangxiong weather station and water level records from Yangzhuyong Co, which show increasing temperature and lower water levels, respectively, since AD 1960. Other studies showed that the water balance for many lakes on the Qinghai-Xizang Plateau is complex, affected by both evaporation and glacial melting. Our paleolimnological reconstructions, which include sediment particle size data, indicate that over relatively short timescales glacial meltwater can influence lake hydrology, but over decadal timescales, increases in evaporation, driven by rising temperatures, dominate. Our findings suggest that regional warming is lowering water levels at these sites and will continue to do so given predicted future climate warming.

Keywords Nam Co · Chen Co · Qinghai-Xizang Plateau · Diatoms · Conductivity · Water balance · Glacial melting · Regional warming

Electronic supplementary material The online version of this article (doi:10.1007/s10933-011-9496-y) contains supplementary material, which is available to authorized users.

R. Wang · X. Yang (✉) · E. Zhang
State Key Laboratory of Lake Science and Environment,
Nanjing Institute of Geography and Limnology, Chinese
Academy of Science, 210008 Nanjing, China
e-mail: xdyang@niglas.ac.cn

R. Wang
e-mail: r.wang@soton.ac.uk

R. Wang · P. Langdon
Palaeoecology Laboratory, Department of Geography,
University of Southampton, Southampton SO17 1BJ, UK

Introduction

Xizang is located on the southern Qinghai-Xizang Plateau, Tibet (Fig. 1), an area dominated by a semi-arid/arid alpine climate, along a geographic gradient from the southeast to northwest. The Plateau region exerts a profound influence on the local weather and climate (Kutzbach et al. 1993; Manabe and Terpstra 1974; Yanai et al. 1992), making it an ideal location

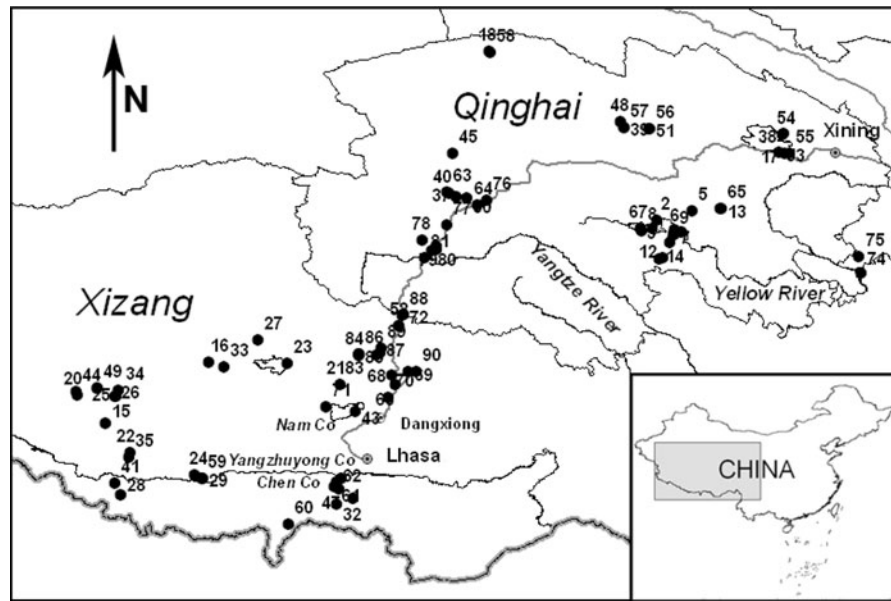


Fig. 1 Location of the study sites on the Qinghai-Xizang Plateau

to test responses to recent climate change. Studies show that most of the Plateau has experienced significant temperature increases during the last few decades (Chen et al. 2003; Liu and Chen 2000). The Plateau is also one of the most sensitive areas to recent temperature increases, as the linear rate of temperature rise between 1955 and 1996 has been about 0.16°C per decade (Liu and Chen 2000), while the global linear warming trend over the 50 years, from 1956 to 2005, has been about 0.13°C per decade (IPCC 2007). IPCC AR4 (2007) suggests that warming of more than 4°C will most likely occur over the Tibetan Plateau by the end of the twenty-first century.

Along with rising temperatures, many lakes in the Plateau region have shrunk to varying degrees, causing an increase in water column ion concentration (Wang et al. 2007; Wang and Dou 1998). Remote sensing studies, however, show that a number of lakes on the middle of the Plateau have expanded recently (Wang et al. 2007; Wu and Zhu 2008; Ye et al. 2007, 2008). Some have argued that the expansion is due to increased glacial melting associated with rising temperatures (Wu and Zhu 2008; Ye et al. 2008), while others have suggested that the balance between precipitation and evaporation (P-E), or Asian summer monsoon variability, is the main reason for the change in lake area (Morrill 2004; Ye et al. 2007). More information is required to

understand the relationships among climate, glaciers and lake hydrology, particularly over long time scales. Unfortunately, there are few instrumental climate datasets from the Qinghai-Xizang Plateau.

In the absence of regular monitoring data, paleolimnology can be an effective tool for understanding past environments (Smol and Cumming 2000). A number of paleolimnological projects have been conducted on the Plateau (Fan et al. 1996; Fontes et al. 1993; Gasse et al. 1991, 1996; Shen et al. 2005; Vancampo and Gasse 1993; Zhu et al. 2009). The majority focused on Holocene/Quaternary hydrologic changes, typically using a combination of diatoms, pollen and geochemistry (Gasse et al. 1991, 1996). Few paleolimnological studies have focused on the recent historical record (Yang et al. 2004), which is crucial to fully understand hydrologic changes in glacially fed lakes over the last century, under rapidly rising temperatures.

Fossil diatom assemblages in lake sediments have been employed to reconstruct past environmental change, and the development of transfer functions has enabled quantitative inferences of climate and hydrochemical variables (Battarbee 1986; Fritz et al. 1991; Gasse and Fourtanier 1991; Gasse et al. 1995; Reed 1998; Stoermer and Smol 1999; Yang et al. 2003). This approach has been used to infer past lake levels and salinity changes (Fritz 1990; Gasse and Fourtanier 1991; Kashima 2003; Roberts and McMinn 1996;

Yang et al. 2004). Such inferences depend on first analyzing a suite of lake surface sediment diatom assemblages and water samples within a geographic region (a training set) to calibrate the diatoms to the environmental variable of interest. Forty lakes on the eastern Tibetan Plateau that represent a broad salinity gradient (0.1–91.7 g/l), were investigated by Yang et al. (2003). Weighted Averaging Partial Least Square (WA-PLS) and Weighted Averaging (WA) regression and calibration models were used independently to establish diatom-based conductivity and water-depth transfer functions (Yang et al. 2003), which were applied to fossil diatom assemblages in a sediment core from Chen Co (Yang et al. 2004).

This paper presents an expanded diatom training set from the Qinghai-Xizang Plateau, based on 90 lakes. The data were used to develop new transfer functions. The transfer functions were applied to the short core from Chen Co again, and a core from Nam Co. Instrumental data were collected close to both sites. Water level records from Yangzhuyong Co and weather data from the Dangxiong station were compared with the down-core reconstructions. Nam Co is the second largest lake on the Qinghai-Xizang Plateau and possesses important pasture lands for the Xizang Autonomous Region within its catchment. Thus, understanding the causes of recent water level changes in Nam Co is crucial for catchment management.

Study region

The new diatom dataset was developed using surface sediment samples from 90 lakes on the Qinghai-Xizang Plateau, which are located between 28° and 39°N and 87°20' and 102°30'E (Fig. 1; Appendix 1—Electronic supplementary material). Their altitudes range from 2,797 to 5,180 m and they are distributed throughout most of the Qinghai-Xizang Plateau (Fig. 1). The Plateau is a high-altitude, arid steppe, interspersed with mountain ranges. It contains thousands of lakes, many of which are large and brackish (Lu et al. 2005; Wang et al. 2007), and is considered one of the most important lake districts in China. Annual precipitation ranges from 278 to 1,158 mm, depending on local elevation and the influence of the Asian summer monsoon (Lu et al. 2005).

Nam Co (30°30'–30°56'N, 90°16'–91°03'E, 4,718 m a.s.l.) is the largest lake in the centre of Tibet (Fig. 1). Regional geology is composed of Mesozoic-group

metamorphite, limestone, granite and Mid-Cenozoic petrosilex. The lake's surface area is ~1,961 km², average depth is 13 m, and maximum depth is >100 m. The lake is brackish and alkaline with a conductivity of 1,800 μS/cm in 2003, pH 9.5, main anion HCO₃⁻ and cation Na⁺ (Wang and Dou 1998). The average annual air temperature is <0°C, with mean monthly temperatures >0°C for only 5 months of the year. The catchment area is about 10,610 km². The lake lies in the hinterland of the Tibetan Plateau. Nyainqentanglha Mountain, to the southeast, provides the main hydrological input from seasonal meltwater. The average elevation of Nyainqentanglha Mountain is about 5,500 m a.s.l., with the highest peak at 7,162 m. According to the Digital Elevation Model (DEM) and satellite images, the glacial area in the catchment was ~167.6 km² in 1970 and ~141.8 km² in 2000. The speed of glacier retreat is about 0.86 km²/a (Wu and Zhu 2008).

Chen Co (28°52'–28°58'N, 90°28'–90°35'E, 4,438 m a.s.l.) is an intermontane basin in Langkazi County on the north slope of the Himalayas, southern Tibet (Fig. 1). The lake has an area of 39.1 km², with a drainage area of 148 km² and is fed by the Kaluxiongqu River. A survey in 1999 showed the deepest part of the lake is >28 m, with pH 9.1 and conductivity 1,024 μS/cm, putting it in the oligosaline range. The lake is adjacent to Yangzhuyong Co, and together these lakes once formed a much bigger water body, with lake terraces dating to before 3.0 ka BP (Li et al. 1982). Climate is thought to have dried thereafter, and the two lakes were separated due to exposure of an underwater delta of the Kaluxiongqu River. The study area is alpine and semi-arid with rainfall mainly concentrated from June to September due to the influence of the summer Indian monsoon. Average annual precipitation is about 370 mm, and annual mean temperature is 2.4°C, while the mean coldest month is January (−5.5°C) and the warmest month is July (9.9°C) (Wang and Dou 1998).

Materials and methods

Diatom dataset

Figure 1 shows the distribution of the 90 study lakes on the Qinghai-Xizang Plateau. Lake sediments and water chemistry samples were collected in the summers of

1998–2005. Sediments were collected from the deepest part of each lake using a Kajak gravity corer. The uppermost 0.5 cm of sediment was subsampled and was assumed to represent the contemporary diatom community of each lake. Slides for diatom analyses were prepared using standard procedures (Battarbee et al. 2001). At least 500 valves were counted from each lake, and diatom communities were described in terms of relative species abundances, i.e. as a percent of the total number of valves counted per lake. Only species with abundance >1% and that appeared in >2 lakes were retained for statistical analysis. Nomenclature and taxonomy mainly followed Krammer and Lange-Bertalot (1988a, b, 1991a, b, 2000), and the current equivalent taxonomy is listed in Appendix 2—Electronic supplementary material.

Water samples (~2 l) were kept at <4°C until analyzed. Chemical analysis included pH, conductivity (cond.), potassium (K⁺), sodium (Na⁺), calcium (Ca²⁺), magnesium (Mg²⁺), chloride (Cl⁻), sulphate (SO₄²⁻), carbonate (CO₃²⁻) and bicarbonate (HCO₃⁻). pH and conductivity were measured in the field, using a HANNA EC-214 pH meter and HI-214 conductivity meter. No analyses of major nutrients were undertaken. Further details of chemical analysis are in Yang et al. (2003).

Sediment cores

In 2003, three short cores (17–25 cm long) were retrieved from a site with water depth of 78 m in Nam Co using a gravity corer. The core site was located in the south-eastern part of the lake, 5 km from the lakeshore to avoid the possibility of collecting slumped deposits. Core stratigraphy was logged in the field (silt throughout) and each core was sampled at 0.5-cm intervals and samples were sealed in plastic bags. The shortest of the three cores (17 cm) was analyzed for diatoms at 0.5-cm intervals from 0 to 10 cm and at 1-cm intervals from 10 to 17 cm. Particle size and organic carbon content were measured at 0.5-cm resolution. Diatom analysis followed methods outlined above for surface samples. Grain size was measured using a laser particle-size analyzer (Master Sizer 2000, Instruments Ltd.) after removal of organic matter with 10% hydrogen peroxide and carbonates with 10% HCl. Medium-diameter (Md) and two other size fractions were considered here: silt particles that represent particle sizes <64 μm, and other particles that will be

considered sand. TOC changed little throughout the profile and hence is not presented.

At Chen Co, a 2.16-m sediment core was obtained from 8 m water depth using a Kajak gravity corer. The core was collected from the gentle slope (~1.5°) on the Kaluxiong River delta. The sediment core was sliced at 1-cm intervals in the field. The profile lithology was comprised of silty mud or clayey silt throughout. Sediment above 45 cm depth was selected for diatom analysis, as preservation was good. Subsamples were analysed at 1-cm intervals from 0 to 30 cm and at 2-cm intervals from 30 to 45 cm. Methods of diatom analysis followed those outlined above, but only 300 valves were counted in each sample from this core. Diatom dissolution can be a problem in saline systems (Fritz 2007). Analyses of these cores indicates that although older sediments are affected by dissolution, during recent decades, the temporal focus of this paper, preservation was not a problem.

Chronology

The top nine cm of the Nam Co core (18 samples, 4–5 g of freeze-dried sediment) was dated using ²¹⁰Pb and ¹³⁷Cs. The activities of ²¹⁰Pb, ²²⁶Ra and ¹³⁷Cs were measured with gamma spectrometry, using a well-type coaxial low background intrinsic germanium detector (Ortec HPGc GWL series). Supported ²¹⁰Pb in each sample was assumed to be in equilibrium with the in situ ²²⁶Ra, and unsupported ²¹⁰Pb (²¹⁰Pb_{exc}) was estimated by subtracting ²²⁶Ra activity from the total ²¹⁰Pb activity (Appleby and Oldfield 1983). The onset of ¹³⁷Cs activity in the core and peak values derived from atmospheric nuclear weapons testing were used to support the ²¹⁰Pb chronology. For Chen Co, we used the chronology derived by Zhu et al. (2003).

Statistical methods

Descriptive statistics and Pearson correlations for environmental variables were calculated using SPSS version 13. Multivariate analyses were employed to examine the relations between environmental variables and diatom communities (Jongman et al. 1995). All environmental variables except pH were normalised by a log(x + 1) transformation to reduce discrepancies between measurement units and reduce the effect of extreme values (Lepš and Šmilauer

2003). Diatom data were square-root transformed to stabilize variance, with rare species down-weighted. Principal component analysis (PCA) was employed to interpret the relations among the environmental variables and detrended correspondence analysis (DCA) was employed to explore the diatom community patterns, as well as to identify the gradient length within the diatom data and hence whether unimodal analyses would be appropriate (ter Braak 1987). A series of canonical correspondence analysis (CCA) tests between diatom species and environmental variables was used to identify the important environmental variables that determine diatom community composition and forward selection and Monte Carlo permutation tests were used to choose possible environmental variables with which to construct diatom-based transfer functions. All numerical analyses mentioned above were completed in CANOCO Version 4.5 (ter Braak and Šmilauer 2002).

Several WA models were tested to develop the best transfer functions, including WA simple, WA_{tot} , and WA-PLS models (Birks et al. 1990; ter Braak and Juggins 1993). The best model was chosen according to the following criteria: the highest R^2 (coefficient of determination) and lowest RMSEP (Root-Mean-Square Error of Prediction) between observed and predicted values in all tested models, and a low mean and a maximum bias. The models were developed using the program CALIBRATE Version 0.70 (Copyright © 1997 S. Juggins and C.J.F. ter Braak).

Results

Training set

Descriptive statistics for environmental variables are shown in Table 1. The conductivity gradient was large, ranging from 100 $\mu\text{S}/\text{cm}$ in Lake DJM03 (S35) to 119,400 $\mu\text{S}/\text{cm}$ in Lake WM205 (S8). pH ranged from 7.4 (KM200, S61) to 11.4 (ZG498, S86) and depth ranged from 0.1 m (XBL03, S44) to 78 m (NMC04, S43). The ranges of conductivity and pH values were similar to the dataset of Yang et al. (2003), but the quantity of lakes at either end of the gradient increased. Figure 2 shows the frequency distribution of conductivity values in this training set. More than 65% of conductivities were $<20,000 \mu\text{S}/\text{cm}$, whereas two lakes (WM205, S8 and DG200, S56) were outliers,

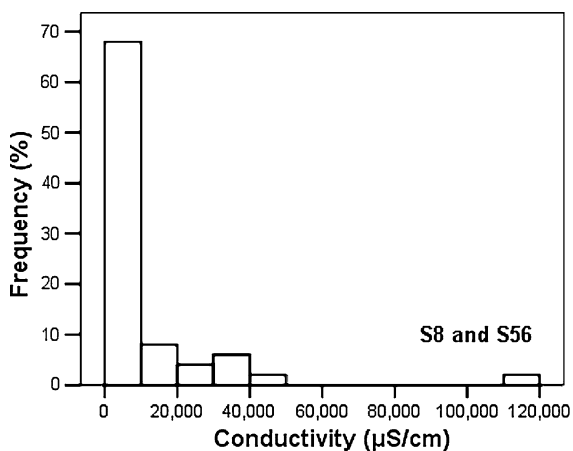
with conductivity values $\sim 120,000 \mu\text{S}/\text{cm}$ (Fig. 2). Lakes S8 and S56 were thus removed from the data set when the diatom-based conductivity model was developed. Correlation coefficients between environmental variables show that conductivity is well correlated with the range of measured ions, with the exception of HCO_3^- and CO_3^{2-} , as expected (Table 1). PCA analysis revealed that there was a pronounced ion concentration gradient in the observed sites, as PCA axis 1 had high correlations with ion concentrations (Table 1), and explained about 69% of the variation among the chemical parameters, more than the 61.8% in the previous dataset. The first two axes explained about 80.4% of the variation and axis 2 has a high correlation only with depth (Table 1).

After removing the outliers and screening for diatoms that only occurred in abundances $>1\%$ and in more than two lakes, 156 diatom species were used for further analysis. Species with high occurrences belonged mainly to littoral epiphytic and benthic freshwater taxa of the genera *Achnanthes* sp., *Amphora* sp., *Cymbella* sp., *Fragilaria* sp. and *Navicula* sp. *Achnanthes minutissima* Kützing appeared in 54 lakes and the maximum percent was 43.3% in TGL98 (S88), which is a small shallow pond, only 0.5 m deep. *Fragilaria pinnata* Ehrenberg, *F. brevistriata* Grunow, *F. construens* f. *venter* (Ehrenberg) Grunow appeared in >30 lakes, and have a very high maximum percentage in the dataset. *Navicula cryptotenella* Kützing was one of the most important species and appeared in 39 lakes. Its maximum percentage was 32.48% in DCC03 (S16), a lake with high pH (10.08) and high conductivity (18,400 $\mu\text{S}/\text{cm}$). *Amphora libyca* Ehrenberg and *A. pediculus* (Kützing) Grunow were also common species, both of which appeared in more than 30 lakes. Meanwhile, centric diatoms were very common on the Qinghai-Xizang Plateau, and included taxa such as *Cyclotella* sp. and *Stephanodiscus minutulus* (Kützing) Cleve & Möller. *Cyclotella ocellata* Pantocsek was very common on the plateau, as it appeared in 45 lakes, with a maximum percentage of 76.2% in YHB03 (S50), a shallow (1 m) lake (conductivity = 1,056 $\mu\text{S}/\text{cm}$). *Stephanodiscus minutulus* and *Cyclostephanos dubius* (Fricke) Round have typically been considered eutrophication indicator species (Adler and Hubener 2007; Ramstack et al. 2003; Yang et al. 2008), although they were found widely throughout the Qinghai-Xizang plateau. *S. minutulus* appeared in 34 lakes, with a maximum

Table 1 Environmental variables and their correlation with conductivity (corr. cond.); the correlations between all environment variables and PCA axes 1 and 2 are also shown

	Minimum	Maximum	Mean	SD	Corr. cond.	PCA AX1	PCA AX2
pH	7.4	11.4	9.1	0.7	−0.08	0.20	−0.23
Cond. (μS/cm)	100	119,400	10,116	19,976	1.00	0.87	0.34
HCO ₃ [−] (mg/l)	0.0	5,623.3	470.6	714.6	0.10	0.31	0.28
CO ₃ ^{2−} (mg/l)	0.0	7,070.7	379.8	842.3	0.14	0.53	0.24
Cl [−] (mg/l)	0.3	68,796.1	4,980.6	13,555.8	0.80	0.82	0.33
SO ₄ ^{2−} (mg/l)	0.2	25,717.4	1,740.7	3,705.7	0.66	0.73	0.44
K ⁺ (mg/l)	0.2	997.2	52.8	154.4	0.41	0.54	0.08
Na ⁺ (mg/l)	0.1	39,631.3	3,609.4	7,837.9	0.73	0.77	0.33
Ca ²⁺ (mg/l)	2.0	2,166.7	83.0	241.6	0.67	−0.05	−0.15
Mg ²⁺ (mg/l)	2.3	28,791.6	998.1	3,355.6	0.39	0.66	0.30
TDS (mg/l)	92.5	122,909.8	12,319.6	26,062.4	0.79	0.77	0.38
Depth (m)	0.1	78.0	8.5	12.5	−0.01	0.09	0.89
Altitude (m a.s.l)	2,797.0	5,180	4,290	609	−0.44	−0.62	−0.08

High correlations, which are significant at $p < 0.01$ (2-tailed) are highlighted in bold

**Fig. 2** Frequency occurrence of sites in the training set in relation to conductivity

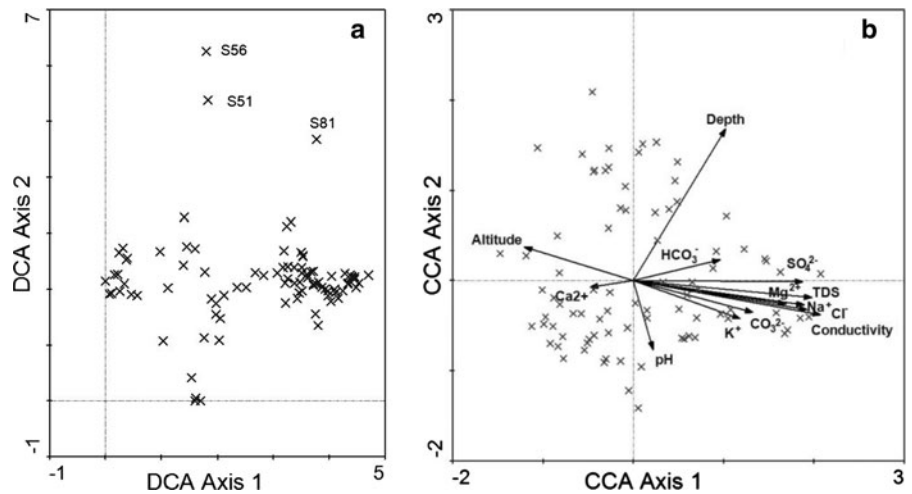
percentage $\sim 90\%$ in LC_03 (S29), a 30-m-deep lake with a conductivity of 2,200 $\mu\text{S}/\text{cm}$. A number of diatom species were found across many lakes on the plateau, but their abundances were not high. Such taxa included *Navicula oblonga* Kützing, *Cymbella leptoceros* (Ehrenberg) Kützing, *Amphora veneta* Kützing, *Cocconeis placentula* var. *lineate* (Ehrenberg) Van Heurck. They were identified in >30 lakes, but with maximum percentages $\sim 10\%$ or less. All diatom species are listed in Appendix 2—Electronic supplementary material.

The first DCA axis for all sites revealed that 4.9% of the variance in the diatom data was explained, and

a gradient length of 4.7 standard deviation (SD) units suggested unimodal methods were appropriate for constrained ordinations. DCA showed that three sites (S51, S56 and S81) were dispersed considerably relative to all other sites (Fig. 3a). S51 (Lake DLH03) and S56 (Lake DG200) were both taken from Delinghagahai Lake, in 2003 and 2000, respectively. The two samples, however, had very different conductivities. S51 yielded a value of 44,700 $\mu\text{S}/\text{cm}$ while S56 was 116,500 $\mu\text{S}/\text{cm}$. The difference was most likely due to samples being taken in different years. S81 (Lake 92_98) is a very small, shallow (0.3-cm-deep) lake, and is located beside a road. These three lakes were deleted from further analysis, due to their identification as outliers under DCA.

An initial CCA with all 13 environmental variables explained 25.3% of the total variance in the diatom community. The first CCA axis explained 6.4% of the diatom distribution through the measured environmental variables, and 4.9% in axis 2. Table 2 shows the marginal and conditional effects of the CCA forward selection results with 13 variables, as well as significant marginal effects of the environmental variables on the diatom assemblages. Conductivity is the most important environmental variable for explaining diatom communities in the dataset (Fig. 3b), and explained about 5.9% of variance in the diatom assemblages. Besides conductivity (and the related ion concentrations), depth and altitude are also

Fig. 3 Ordination plots showing: **a** DCA with all sites (90) and **b** CCA with 87 sites (without S51, S56 and S81)



significant for the distribution of diatom assemblages (Fig. 3b), and explained 4.7 and 3.3% of the variance in diatom assemblages, respectively. pH had no significant effect on the diatom assemblages in this dataset. The conditional effects are displayed in Table 2 and indicate that depth and altitude can independently be significant to diatom communities. A CCA analysis using automatic selection with the best $K = 3$ variables and Monte Carlo Permutation Tests indicated that conductivity, depth and altitude explained 6.2% of the variance in the diatom assemblages. Further analysis using only individual environmental variables in CCA showed that λ_1/λ_2 (0.97) for conductivity was high enough to generate a diatom-based conductivity transfer function using WA methods (Gregory-Eaves et al. 1999; Wunsam et al. 1995; Reavie et al. 1995; Hall and Smol 1996; Chen et al. 2008). We therefore focused on inferring conductivity from diatom assemblages in this paper.

Diatom-based conductivity transfer functions

Several WA models were generated to construct a diatom-based conductivity transfer function (Table 3). Results for the conductivity model were different from the previous training set (Yang et al. 2003), which showed that a WA-PLS(2) model produced the best performance statistics ($r_{jack}^2 = 0.92$; $RMSEP_{jack} = 0.22$). Analysis here showed that the WA-partial least squares regression method did not improve the predictive ability compared with a simple WA model (Table 3). It is likely that expanding the conductivity range in this dataset ensured that this was

the variable with the dominant environmental gradient on the Qinghai-Xizang plateau, similar to the approaches taken when measuring diatom community trophic status optima in the lower Yangtze River catchment (Yang et al. 2008). For this new training set, WA with classical deshrinking produced the highest r_{jack}^2 (0.74), while WA with inverse deshrinking gave the lowest predictive errors ($RMSEP_{jack} = 0.37$). The results indicated that inverse deshrinking gave a lower overall predictive error while classical deshrinking resulted in a better fit of estimated versus observed values (Birks et al. 1990; ter Braak and Juggins 1993; Yang et al. 2008). Adding sites produced a lower r_{jack}^2 than before, and made the $RMSEP_{jack}$ higher, which is a common consequence of expanding the number of sites in training sets (Walker and Cwynar 2006). Model results show that observed versus predicted conductivity displayed a reasonably good match (Fig. 4a). The residuals (Fig. 4b) showed that conductivities in some freshwater lakes were overestimated, and conductivities in some hypersaline lakes were underestimated.

Sediment cores

Chronology

The ^{210}Pb data for the upper part of the Chen Co core was published by Zhu et al. (2003). The average deposition rate from 0 to 45 cm depth was ~ 1.64 mm/a. The ^{210}Pb activities for Nam Co declined exponentially with depth (Fig. 5). Calculated ages were similar between the Constant Rate of Supply

Table 2 CCA forward selection results with 13 variables and significant marginal effects of environmental variables on the diatom assemblages

Marginal effects		Variance explained	Conditional effects			
Variable	λ_1		Variable	λ_A	P	F
Conductivity	0.40	5.9	Conductivity	0.40	0.001	5.22
TDS	0.37	5.5	Depth	0.29	0.001	4.05
Cl ⁻	0.36	5.3	Altitude	0.16	0.001	2.12
Na ⁺	0.36	5.3	Ca ²⁺	0.13	0.001	1.88
SO ₄ ²⁻	0.34	5.0	TDS	0.10	0.006	1.44
Depth	0.32	4.7	SO ₄ ²⁻	0.10	0.056	1.31
Mg ²⁺	0.30	4.4	CO ₃ ²⁻	0.09	0.09	1.24
CO ₃ ²⁻	0.23	3.3	HCO ₃ ⁻	0.08	0.12	1.24
Altitude	0.23	3.3	Mg ²⁺	0.10	0.036	1.33
K ⁺	0.20	3.0	K ⁺	0.08	0.156	1.17
HCO ₃ ⁻	0.15	2.2	Cl ⁻	0.07	0.344	1.04
Ca ²⁺	0.13	2.0	Na ⁺	0.07	0.559	0.95
pH	0.10	Not significant	pH	0.05	0.874	0.8

Table 3 Summary of models tested for the new diatom-based transfer functions

Parameter	Model	RMSEP _{jack}	r _{jack} ²	Mean bias	Max bias
Conductivity	<i>Inverse</i>				
	WA	0.37	0.74	0.00	0.55
	WA _{tot}	0.37	0.73	-0.01	0.53
	<i>Classical</i>				
	WA	0.38	0.74	0.00	0.43
	WA _{tot}	0.38	0.74	-0.02	0.44
	WA-PLS (1)	0.37	0.74	0.00	0.55
	WA-PLS (2)	0.39	0.71	0.03	0.37
	WA-PLS (3)	0.47	0.63	0.06	0.49
	WA-PLS (4)	0.55	0.54	0.08	0.61

(CRS) and Constant Initial Concentration (CIC) models. The CIC results showed the sediment accumulation rate was about 0.833 mm/a, with an age at 17 cm depth of about AD 1805. The first appearance of ¹³⁷Cs at 4.75 cm was related to the onset of global nuclear testing in 1952, and this age coincides with the results from ²¹⁰Pb dating (CIC model) (Fig. 5). A peak ¹³⁷Cs value of 20–22.5 Bq/kg at 2.25–2.75 cm may correspond to peaks in nuclear

weapons testing from 1963 and 1972, documented in China (Zhu et al. 2003). In this core, the sedimentation rate from the ²¹⁰Pb model suggests the ¹³⁷Cs peak corresponds to a date of 1972.

Fossil diatoms

A total of 65 diatom species were recorded in the Nam Co core, 43 of them present in the Qinghai-Xizang calibration set. All the abundant fossil species were present in the surface sediment dataset. Fossil diatoms were characterised by abundant planktonic taxa, with *Cyclotella ocellata* Pantocsek contributing 40–80% of the total count sum throughout the core (Fig. 6). *Stephanodiscus minutulus* (Kützing) Cleve & Möller and *Aulacoseira ambigua* (Grunow) Simonsen were particularly abundant in the top 3.5 cm and in the interval from 11 to 14 cm. Littoral and benthic taxa such as *F. brevistriata* Grunow, *F. pinnata* Ehrenberg, *Amphora pediculus* (Kützing) Grunow, *A. ovalis* (Kützing) Kützing, *Achmanthes clevei* Grunow, and *Navicula oblonga* Kützing, were also present, but less dominant. Four diatom zones with two sub-zones were identified based on changes in species abundance. The basal zone 1 (17–14 cm) had *Cyclotella ocellata* as the sole dominant species (60–83%) with only a few non-planktonic species, such as *A. ovalis*, *Epithemia argus* (Ehrenberg) Kützing and *Navicula oblonga* present in this zone.

Fig. 4 Plots of observed versus predicted log-transformed conductivity as well as depth and of the residuals (inferred–observed). **a** Plot of observed conductivity versus predicted conductivity by WA classical deshrinking without tolerance down-weighting, **b** is the residuals for the respective models

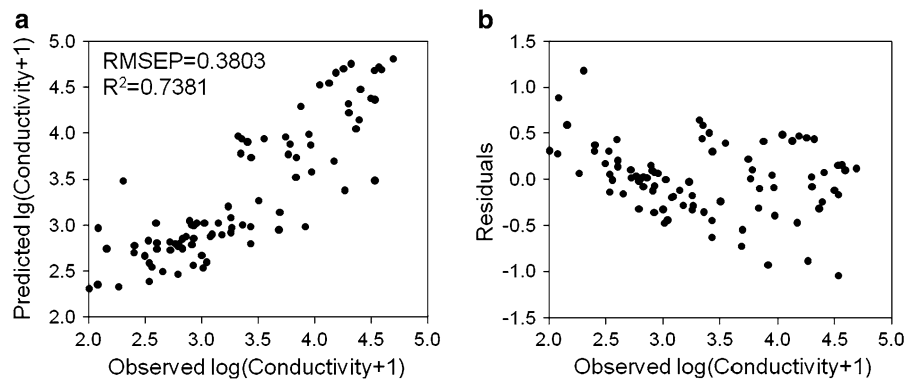
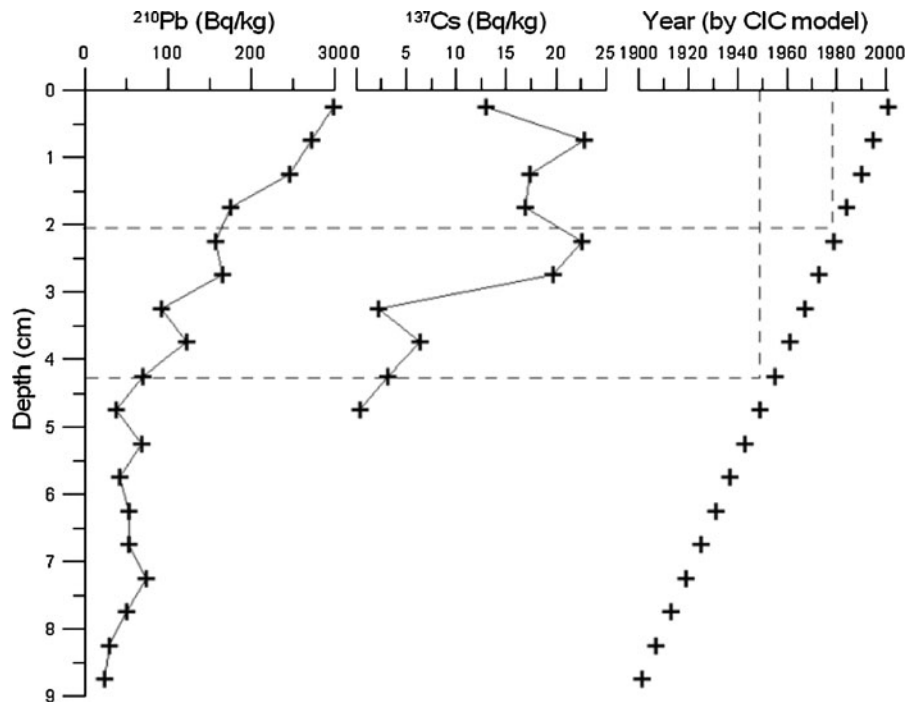


Fig. 5 ²¹⁰Pb and ¹³⁷Cs activity profiles for the Nam Co sediment core. Dates were calculated using the ²¹⁰Pb CIC model



Zone 2 (14–11 cm) was characterised by increasing values for *Aulacoseira ambigua* (8–30%) and decreasing values for *Cyclotella ocellata* (40% at 11.5 cm). Other species were rare in this zone. In zone 3 (11–3.5 cm), *Cyclotella ocellata* again became the dominant species (60–72%), although the percentages were slightly lower than those recorded in zone 1. Values for *Aulacoseira ambigua* were seen to decrease significantly in this zone, with values falling to <10%. Significant changes occurred in zone 4, above 3.5 cm, with *Cyclotella ocellata* decreasing from 60 to 40%, while *Stephanodiscus minutulus* increased gradually to a peak of 35% at the

top of the record. *Amphora pediculus* was the sub-dominant species in this zone (10–15%). Even though the abundance of other planktonic and non-planktonic species in the samples was low, a distinct spike in the values of *Aulacoseira ambigua* and *Fragilaria brevistriata*, as well as *Amphora pediculus*, can be seen between 3 and 2 cm.

Fossil diatoms in Chen Co were presented by Yang et al. (2003). Diatom assemblages were characterized by epiphytic *Amphora ovalis*, *Gyrosigma acuminatum* (Kützing) Rabenhorst and *Campylodiscus noricus* Ehrenberg, accompanied by small amounts of *Cymbella ehrenbergii* Kützing and *Diploneis elliptica*

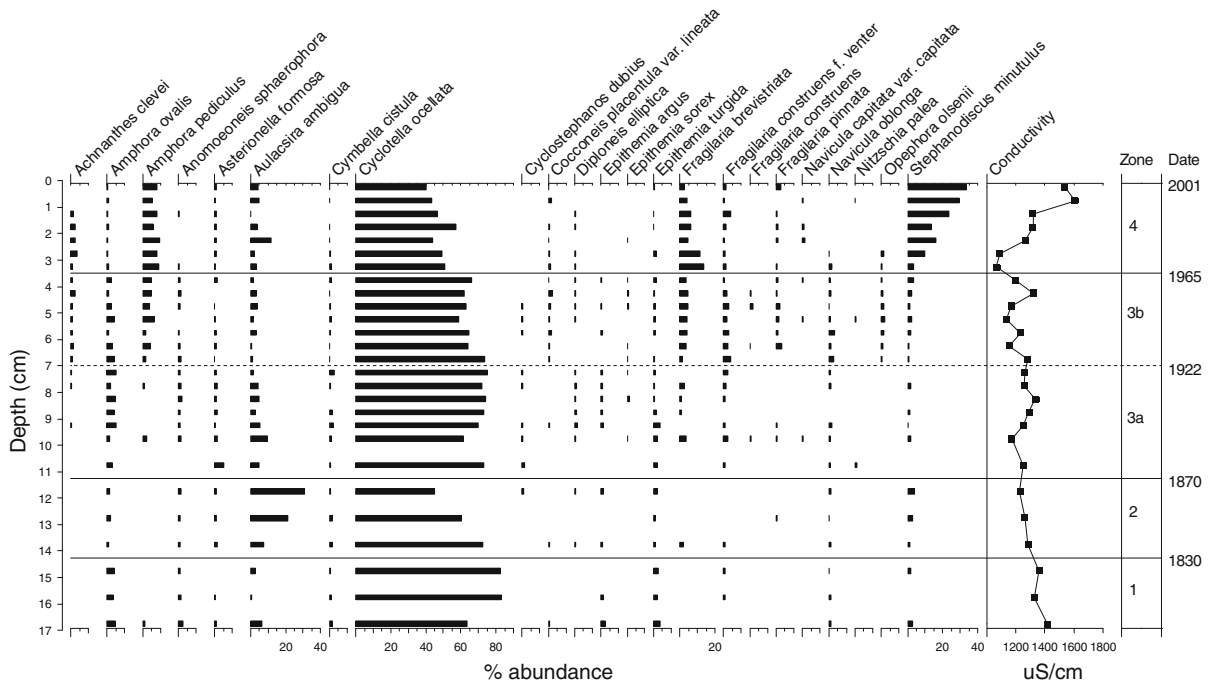


Fig. 6 Fossil diatom assemblages in the Nam Co core

(Kützing) Cleve, at the bottom of the core. *Cyclotella ocellata* and *C. bodanica* Grunow, increased with the occurrences of some benthic taxa such as *Fragilaria* types and *Mastogloia smithii* Thwaites. Together they constituted the dominant species of the middle of the core. At the top of the core the diatom assemblage shifted from the former dominant species to benthic and littoral *Amphora pediculus*, *Nitzschia perminuta* (Grunow) M. Peragallo and *Cocconeis placentula* Ehrenberg. The centric *Cyclotella* types decreased in relative terms, but still maintained high numbers.

Diatom-inferred conductivity and sediment grain size

Diatom-inferred conductivity for both the Chen Co and Nam Co cores is shown in Fig. 7. The conductivity of Nam Co was stable, with few fluctuations between the 1800s and 1960s, when the diatom-inferred conductivity was $\sim 1,300 \mu\text{S}/\text{cm}$. The conductivity, however, increased significantly during the past 40 years, from a value around $1,200 \mu\text{S}/\text{cm}$ in 1960, to $1,600 \mu\text{S}/\text{cm}$ in 2000. Directly measured conductivity was $1,800 \mu\text{S}/\text{cm}$ in 2003. In comparison, diatom-inferred conductivity changes in Chen Co were even greater during the past 200 years.

Inferred conductivity decreased from $800 \mu\text{S}/\text{cm}$ in 1810 to $500 \mu\text{S}/\text{cm}$ in 1830. It then increased a little during the next 100 years, when the values fluctuated around $700 \mu\text{S}/\text{cm}$. Chen Co's conductivity increased substantially over the past 30 years, but there was a year of decrease in 1986. In general, the conductivity trajectory during past 200 years for both lakes is similar, illustrating a slight decrease at the start of period, followed by an increasing trend in the following decades, and increasing substantially in the last 40 years.

Sediment particle size in Nam Co is also shown in Fig. 7, illustrating silt-size (Fig. 7c), sand-size (Fig. 7d) and median-size grains (Fig. 7e). Relations can be seen among particle sizes. The percent silt decreased after the 1880s, whereas there was an increase in both the coarse and median-sized sediment grains.

Discussion and conclusions

We focused on expanding the Qinghai-Xizang diatom training set from 40 to 90 lakes and applied the resultant transfer function to recent lake sediment

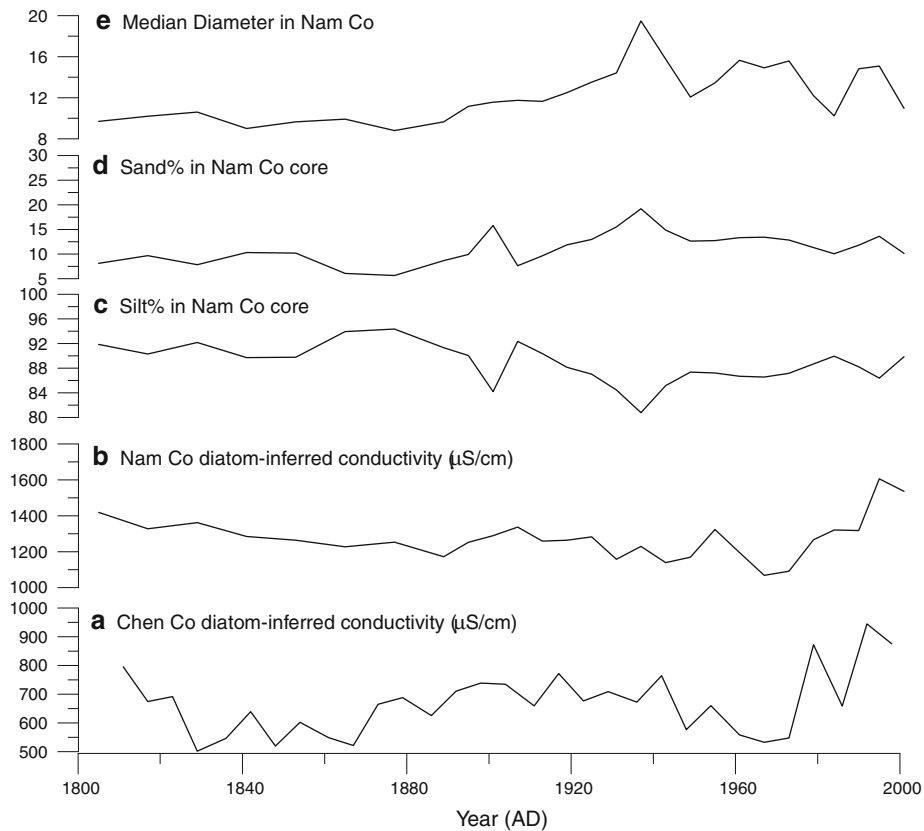


Fig. 7 Diatom-inferred conductivity reconstructions for Chen Co (a) and Nam Co (b); c silt particles <64 μm in Nam Co; d sand particles >64 μm in Nam Co; e median diameter of sediment particles in Nam Co

sequences from Xizang. Conductivity is the most important variable in explaining diatom distributions. Water depth is also significant. The fossil diatom community in Nam Co was dominated by *C. ocellata* throughout the core, but *S. minutulus* became important in very recent deposits (Fig. 6). This latter species is typically indicative of fresh water eutrophication (Adler and Hubener 2007; Ramstack et al. 2003; Yang et al. 2008), hence one interpretation is that the increasing abundance of *S. minutulus* was due to freshwater input into Nam Co. *S. minutulus*, however, occurred in 34 lakes of the new training set, illustrating how widely distributed it is on the Qinghai-Xizang Plateau. Figure 8 shows its normal distribution of abundance across the conductivity gradient. Optimum conductivity calculated by the WA classical model for this species was 2,110 μS/cm, which is quite different from its optima in other datasets, such as western North American (salinity optimum: 0.21 g/l) (Wilson et al. 1996) and

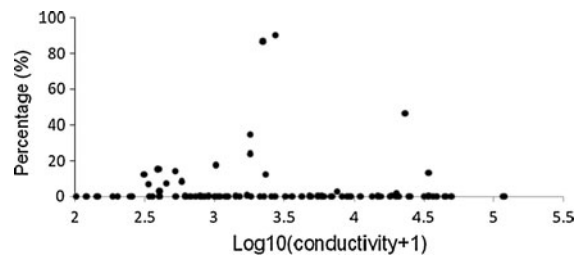


Fig. 8 Conductivity versus *Stephanodiscus minutulus* relative abundance in the new Qinghai-Xizang lake dataset

Africa (conductivity optimum: 131.8 μS/cm) (Gasse et al. 1995). Our results suggest this taxon is a brackish species on the Qinghai-Xizang Plateau. It had a much higher conductivity optimum than *Cyclotella ocellata* which had a conductivity optimum of 1,552 μS/cm. Our interpretation is that *S. minutulus* occupies a different habitat on the Qinghai-Xizang Plateau compared with *Stephanodiscus* sp. in other

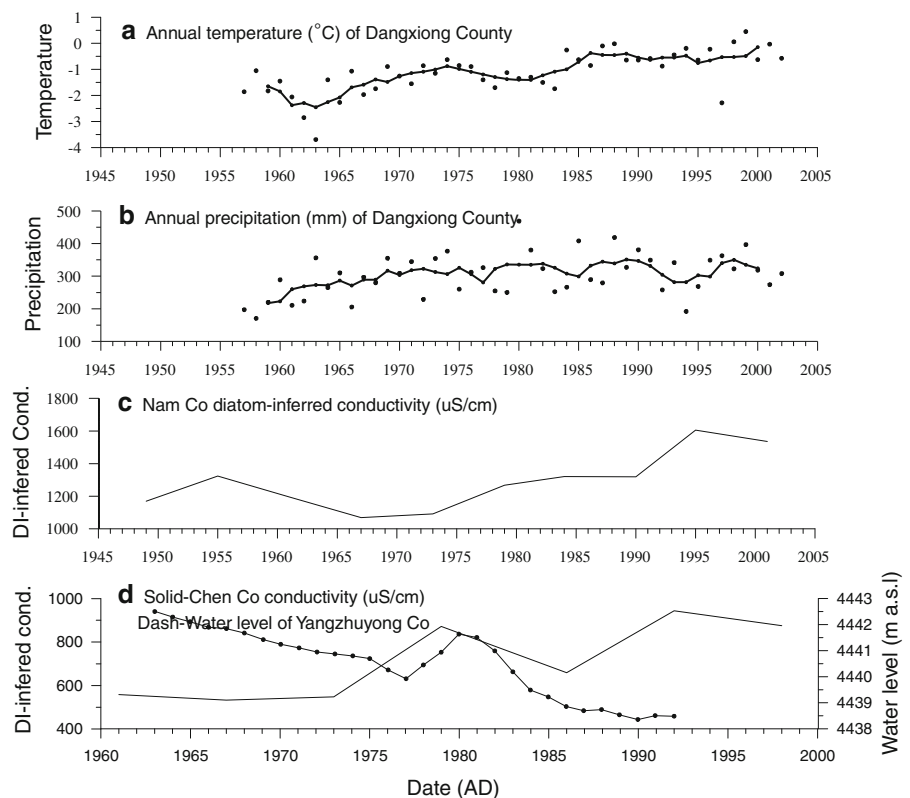
areas (Adler and Hubener 2007; Ramstack et al. 2003; Yang et al. 2008). In this semi-arid region, the distribution of *Stephanodiscus* sp. mainly depends on the ionic concentration in the lakes, and our data indicate that it prefers brackish water. Therefore, in Nam Co, increased abundance of *S. minutulus* likely indicates the rise of lake conductivity and the associated decline of lake volume in recent decades, rather than additional water input.

The conductivity reconstruction for Chen Co showed similar trends in the past 200 years to that of Nam Co, although the Nam Co profile is much less variable than that of Chen Co. One reason could be that Nam Co is much larger than Chen Co and hence relatively more stable over decadal to centennial timescales. Verification of these reconstructions is difficult, however, because there are few measured water chemistry datasets from this region. Whereas the balance between precipitation and evaporation (P-E) can be the main factor that determines water balance in arid or semi-arid areas, and lake evaporation is mainly controlled by air temperature, the relation between temperature and precipitation can also determine the

water balance in such regions. To test this, the climate data from Dangxiong weather station, near Nam Co (Fig. 1) and water level changes in Yangzhuyong Co, were compared with the reconstructions. Figure 9a illustrates the recent warming on the Qinghai-Xizang Plateau, but the precipitation changes during the past 40 years (1957–2003) show little overall trend. These data suggest that evaporation likely increased in this region during this period, and hence negative water balance caused lake conductivity to rise. Both reconstructions in Nam Co and Chen Co showed an increase in conductivity, with fluctuations during the past 40 years (Fig. 9c, d). Both the Chen Co conductivity reconstruction and water level records from nearby Yangzhuyong Co (Fig. 9d) show evidence for drying, especially around 1980. These comparisons with instrumental data suggest that the conductivity reconstructions are likely accurate in both lakes.

Water balance on the Qinghai-Xizang plateau, however, is not controlled solely by precipitation and evaporation, but is also strongly affected by glacial meltwater. A main water source for Nam Co is meltwater from Nyainqentanglha Mountain. Figure 7e

Fig. 9 Comparisons between diatom-inferred conductivity and measured data: **a** annual temperature (°C) of Dangxiong County (5-point running mean); **b** annual precipitation (mm) of Dangxiong County (5-point running mean); **c** diatom-inferred conductivity (µS/cm) in Nam Co; **d** diatom-inferred conductivity (µS/cm) in Chen Co (solid line) and Yangzhuyong Co water level change (dashed line)



shows that the median- and sand-size particle grains in the sediment increased over the last century, while the silt-size particles decreased in relative abundance, suggesting a general enhancement of flow into Nam Co, though both reconstructions show a slight decrease in inflow during the 1920s–1940s (Fig. 7). Increased input might have been due to an increase in meltwater as climate in the region warmed. This increase in meltwater, in turn, increased discharge to the lake, thereby diluting the ionic strength of the lake water. After the 1940s, particle size was stable (Fig. 7c, d), but the lake likely received increased glacial meltwater thereafter, as the glacier in the Nam Co catchment has been shrinking since the 1970s, and possibly longer. Unfortunately, there are no data before this period. Yao et al. (2007) showed that the glacial area was about 167.6 km² in 1970, 151.5 km² in 1990, and 141.8 km² in 2000, which means that glacial retreat rate was around 0.81 km²/a from 1970 to 1990, and ~0.97 km²/a in the 1990s. Although an increase in meltwater could lead to a freshening of the lake, greater meltwater input occurred during a period of warming climate. Our data show that the conductivity of the lake increased during this period, indicating that the lake water budget declined over this time span. We conclude that evaporation, driven by an increase in summer temperatures, was a more important process than increased melt water discharge, and hence the lake shrunk in recent decades.

Remote sensing studies have shown that many lakes on the middle of the Plateau expanded recently (Wang et al. 2007; Wu and Zhu 2008; Ye et al. 2007, 2008), and this was thought to have been due to increasing glacial melting. In such a complex system, however, changing lake water levels are unlikely to be affected solely by one factor. During regional warming, temperature increases enhance evaporation as well as glacial melting, and contribute to fluctuating lake levels. Understanding the timing and nature of these oscillations is crucial for lake management and for understanding the relations between climate change and lake hydrology. Although remote sensing can be used to identify hydrologic changes over annual or even monthly timeframes, it cannot be used to determine longer-term fluctuations. Paleolimnological techniques can fill this data gap. Ultimately, however, we recommend that both approaches be used to fully understand the historical hydrologic trajectory of a lake.

Figures 7a and b indicate that conductivity in both Nam Co and Chen Co has increased during the past 40 years. One could argue that the lakes are shrinking over longer time scales due to regional warming, but the lakes have fluctuated during this period because of increases in glacial meltwater. It is likely that increasing evaporation, through rising temperatures, is the dominant control on lake water levels at the decadal scale. Glacial meltwater, delivered at a higher rate in recent years as a consequence of warming, is causing lake level fluctuations at shorter temporal scales, but has not shifted the directional trend of lake level change over longer timescales.

Acknowledgments This study was supported by the National Basic Research Program of China (973 program, 2010CB950201) and the National Science Foundation of China (Grant No. 40772204). We are grateful to Dr. Yanling Li for help with diatom identification, to Weilan Xia for ²¹⁰Pb dating, and to Hongxi Pan for chemical measurements. We particularly thank Richard Jones, Roland Schmidt, and two anonymous referees for their helpful comments on this study.

References

- Adler S, Hubener T (2007) Spatial variability of diatom assemblages in surface lake sediments and its implications for transfer functions. *J Paleolimnol* 37:573–590
- Appleby PG, Oldfield F (1983) The assessment of Pb-210 data from sites with varying sediment accumulation rates. *Hydrobiologia* 103:29–35
- Battarbee RW (1986) Diatom analysis. In: Berglund BE (ed) *Handbook of Holocene palaeoecology and palaeohydrology*. Wiley, Chichester, pp 527–570
- Battarbee RW, Jones VJ, Flower RJ, Cameron NG, Bennion H (2001) Diatoms. In: Smol JP, Birks HJB, Last WM (eds) *Tracking environmental change using lake sediments*. Kluwer, Dordrecht, pp 172–176
- Birks HJB, Line JM, Juggins S, Stevenson AC, ter braak CJF (1990) Diatoms and pH reconstruction. *Philos Trans R Soc B* 327:263–278
- Chen B, Chao WC, Liu X (2003) Enhanced climatic warming in the Tibetan Plateau due to doubling CO₂: a model study. *Clim Dyn* 20:401–413
- Chen GJ, Dalton C, Leira M, Taylor D (2008) Diatom-based total phosphorus (TP) and pH transfer functions for the Irish Ecoregion. *J Paleolimnol* 40:143–163
- Fan H, Gasse F, Huc A, Li YF, Sifeddine A, Soulie-Marsche I (1996) Holocene environmental changes in Bangong Co basin (western Tibet). 3. biogenic remains. *Palaeogeogr Palaeoclimatol Palaeoecol* 120:65–78
- Fontes JC, Melieres F, Gibert E, Qing L, Gasse F (1993) Stable-isotope and radiocarbon balances of two Tibetan Lakes (Sumxi Co, Longmu Co) from 13,000-BP. *Quat Sci Rev* 12:875–887

- Fritz SC (1990) 20th-century salinity and water-level fluctuations in Devils Lake, North-Dakota—test of a diatom-based transfer-function. *Limnol Oceanogr* 35:1771–1781
- Fritz SC (2007) Salinity and climate reconstruction from diatoms in continental lake deposits. In: Elias S (ed) *Encyclopedia of quaternary science*, vol 1. Elsevier, Oxford, pp 514–522
- Fritz SC, Juggins S, Battarbee RW, Engstrom DR (1991) Reconstruction of past changes in salinity and climate using a diatom-based transfer-function. *Nature* 352:706–708
- Gasse F, Fourtanier E (1991) African diatom paleoecology and biostratigraphy. *J Afr Earth Sci* 12:325–334
- Gasse F, Arnold M, Fontes JC, Fort M, Gibert E, Huc A, Li BY, Li YF, Liu Q, Mélières F, Vancampo E, Wang FB, Zhang QS (1991) A 13,000-year climate record from western Tibet. *Nature* 353:742–745
- Gasse F, Juggins S, Khelifa LB (1995) Diatom-based transfer functions for inferring past hydrochemical characteristics of African lakes. *Palaeogeogr Palaeoclimatol* 117:31–54
- Gasse F, Fontes JC, VanCampo E, Wei K (1996) Holocene environmental changes in Bangong Co basin (western Tibet). 4. discussion and conclusions. *Palaeogeogr Palaeoclimatol* 120:79–92
- Gregory-Eaves I, Smol JP, Finney BP, Edwards ME (1999) Diatom-based transfer functions for inferring past climatic and environmental changes in Alaska, USA. *Arct Antarct Alp Res* 31:353–365
- Hall RI, Smol JP (1996) Paleolimnological assessment of long-term water-quality changes in south-central Ontario lakes affected by cottage development and acidification. *Can J Fish Aquat Sci* 53:1–17
- IPCC (2007) *Climate change 2007: synthesis report*. Contribution of working groups I, II and III to the fourth assessment report of the Intergovernmental Panel on Climate Change [Core Writing Team, Pachauri RK, Reisinger A (eds)]. IPCC, Geneva, Switzerland, 104 pp
- Jongman RH, ter Braak CJF, Van Tongeren OFR (1995) *Data analysis in community and landscape ecology*. Cambridge University Press, Cambridge, 299 pp
- Kashima K (2003) The quantitative reconstruction of salinity changes using diatom assemblages in inland saline lakes in the central part of Turkey during the Late Quaternary. *Quat Int* 105:13–19
- Krammer K, Lange-Bertalot H (1988a) *Bacillariophyceae*. 2 Teil, Bacillariaceae, Epithemiaceae, Surirellaceae. Gustav Fischer, Stuttgart 596 pp
- Krammer K, Lange-Bertalot H (1988b) *Bacillariophyceae*. 2/1 Teil, Naviculaceae. Gustav Fischer, Stuttgart 876 pp
- Krammer K, Lange-Bertalot H (1991a) *Bacillariophyceae*. 3 Teil, Centrales, Fragilariaceae, Eunotiaceae. Gustav Fischer, Stuttgart 576 pp
- Krammer K, Lange-Bertalot H (1991b) *Bacillariophyceae*. 4 Teil, Achnantheaceae, Kritische Ergänzungen zu Navicula (Lineolatae) und Gomphonema Gesamtliteraturverzeichnis Teil 1–4. Gustav Fischer, Stuttgart 437 pp
- Krammer K, Lange-Bertalot H (2000) *Bacillariophyceae*. Part 5, English and French translation of the keys. *Spectrum*, Heidelberg 311 pp
- Kutzbach JE, Prell WL, Ruddiman WF (1993) Sensitivity of Eurasian climate to surface uplift of the Tibetan Plateau. *J Geol* 101:177–190
- Lepš J, Šmilauer P (2003) *Multivariate analysis of ecological data using CANOCO*. Cambridge University Press, Cambridge 269 pp
- Li BY, Wang FB, Yang YC, Zhang QS (1982) On the paleogeographical evolution of Xizang (Tibet) in the Holocene. *Geogr Res* 1:26–36
- Liu XD, Chen BD (2000) Climatic warming in the Tibetan Plateau during recent decades. *Int J Climatol* 20:1729–1742
- Lu CX, Yu G, Xie GD (2005) Tibetan plateau serves as a water tower. *IGARSS 2005: IEEE international geoscience and remote sensing symposium*, pp 3120–3123
- Manabe S, Terpstra TB (1974) Effects of mountains on general circulation of atmosphere as identified by numerical experiments. *J Atmos Sci* 31:3–42
- Morrill C (2004) The influence of Asian summer monsoon variability on the water balance of a Tibetan lake. *J Paleolimnol* 32:273–286
- Ramstack JM, Fritz SC, Engstrom DR, Heiskary SA (2003) The application of a diatom-based transfer function to evaluate regional water-quality trends in Minnesota since 1970. *J Paleolimnol* 29:79–94
- Reavie ED, Hall RI, Smol JP (1995) An expanded weighted-averaging model for inferring past total phosphorus concentrations from diatom assemblages in Eutrophic British-Columbia (Canada) lakes. *J Paleolimnol* 14:49–67
- Reed JM (1998) A diatom-conductivity transfer function for Spanish salt lakes. *J Paleolimnol* 19:399–416
- Roberts D, McMinn A (1996) Relationships between surface sediment diatom assemblages and water chemistry gradients in saline lakes of the Vestfold Hills, Antarctica. *Antarct Sci* 8:331–341
- Shen J, Liu XQ, Wang SM, Matsumoto R (2005) Palaeoclimatic changes in the Qinghai Lake area during the last 18,000 years. *Quatern Int* 136:131–140
- Smol JP, Cumming BF (2000) Tracking long-term changes in climate using algal indicators in lake sediments. *J Phycol* 36:986–1011
- Stoermer EF, Smol JP (1999) *The diatoms: applications for the environmental and earth sciences*. Cambridge University Press, Cambridge, 469 pp
- ter Braak CJF (1987) The analysis of vegetation-environment relationships by canonical correspondence-analysis. *Plant Ecol* 69:69–77
- ter Braak CJF, Juggins S (1993) Weighted Averaging Partial Least-Squares Regression (WA-PLS)—an improved method for reconstructing environmental variables from species assemblages. *Hydrobiologia* 269:485–502
- ter Braak CJF, Šmilauer P (2002) *CANOCO reference manual and CanoDraw for windows user's guide: software for canonical community ordination (version 4.5)*. Microcomputer Power, Ithaca. www.canoco.com
- Vancampo E, Gasse F (1993) Pollen-inferred and diatom-inferred climatic and hydrological changes in Sumxi Co basin (Western Tibet) since 13,000 yr BP. *Quat Res* 39:300–313
- Walker IR, Cwynar LC (2006) Midges and palaeotemperature reconstruction—the North American experience. *Quat Sci Rev* 25:15
- Wang SM, Dou HS (1998) *Lakes in China*. Science Press, Beijing (in Chinese)

- Wang LH, Lu AX, Yao TD, Wang NL (2007) The study of typical glaciers and lakes fluctuations using remote sensing in Qinghai-Tibetan Plateau. *Int Geosci Remote Sens* 45:26–4529
- Wilson SE, Cumming BF, Smol JP (1996) Assessing the reliability of salinity inference models from diatom assemblages: an examination of a 219-lake data set from western North America. *Can J Fish Aquat Sci* 53:1580–1594
- Wu YH, Zhu LP (2008) The response of lake-glacier variations to climate change in Nam Co Catchment, central Tibetan Plateau, during 1970–2000. *J Geogr Sci* 18:177–189
- Wunsam S, Schmidt R, Klee R (1995) *Cyclotella-taxa* (Bacillariophyceae) in lakes of the Alpine region and their relationship to environmental variables. *Aquat Sci* 57:360–386
- Yanai MH, Li CF, Song ZS (1992) Seasonal heating of the Tibetan Plateau and its effects on the evolution of the Asian summer monsoon. *J Meteorol Soc Jpn* 70:319–351
- Yang XD, Kamenik C, Schmidt R, Wang SM (2003) Diatom-based conductivity and water-level inference models from eastern Tibetan (Qinghai-Xizang) Plateau lakes. *J Paleolimnol* 30:1–19
- Yang XD, Wang SM, Kamenik C, Schmidt R, Shen J, Zhu LP, Li SF (2004) Diatom assemblages and quantitative reconstruction for paleosalinity from a sediment core of Chencuo Lake, southern Tibet. *Sci China Ser D* 47:522–528
- Yang XD, Anderson NJ, Dong XH, Shen J (2008) Surface sediment diatom assemblages and epilimnetic total phosphorus in large, shallow lakes of the Yangtze floodplain: their relationships and implications for assessing long-term eutrophication. *Freshw Biol* 53:1273–1290
- Yao T, Pu J, Lu A, Wang Y, Yu W (2007) Recent glacial retreat and its impact on hydrological processes on the Tibetan plateau, China, and surrounding regions. *Arct Antarct Alp Res* 39:642–650
- Ye QH, Zhu LP, Zheng HP, Naruse RJ, Zhang XQ, Kang SC (2007) Glacier and lake variations in the Yamzhog Yumco basin, southern Tibetan Plateau, from 1980 to 2000 using remote-sensing and GIS technologies. *J Glaciol* 53:673–676
- Ye QH, Yao TD, Chen F, Kang SC, Zhang XQ, Wang Y (2008) Response of glacier and lake covariations to climate change in Mapam Yumco basin on Tibetan plateau during 1974–2003. *J China Univ Geosci* 19:135–145
- Zhu LP, Zhang PZ, Xia WL, Li BY, Chen L (2003) 1400-year cold/warm fluctuations reflected by environmental magnetism of a lake sediment core from the Chen Co, southern Tibet, China. *J Paleolimnol* 29:391–401
- Zhu LP, Zhen XL, Wang JB, Lu HY, Xie MP, Kitagawa H, Possnert G (2009) A similar to 30,000-year record of environmental changes inferred from Lake Chen Co, Southern Tibet. *J Paleolimnol* 42:343–358